EUROPEAN ORGANIZATION FOR NUCLEAR RESEARCH

CERN-EP/2001-037
CERN-SL-2001-016 EA

CNGS: effects of possible alignment errors

A.E. Ball[1], **A. Guglielmi**[2], **F. Pietropaolo**[1*],
P.R. Sala[1†], **N. Vassilopoulos**[1], **H. Vincke**[1]

[1] *CERN, CH-1211 Geneva 23, Switzerland*
[2] *INFN, Sezione di Padova, Via Marzolo 8, I-35131, Padova, Italy*

Abstract

Simulations of the CNGS neutrino beam from CERN to the Gran Sasso Laboratory (LNGS) assume that the proton beam and all secondary beam elements are perfectly aligned on an axis between the two laboratories. This study examines the effects on the neutrino flux at Gran Sasso of deviations from the axis of the primary proton beam and misalignment of secondary beam elements. It also examines how such deviation or misalignment can be detected at monitors placed along the secondary beam line at CERN and at Gran Sasso. Calculations are based on the CNGS neutrino beam, optimized for $\nu_\mu \rightarrow \nu_\tau$ appearance experiments as described in the Addendum to the Conceptual Technical Design Report of CNGS. It is shown that the number of neutrino charged current events predicted at Gran Sasso is insensitive to all but the most extreme misalignments.

To be submitted to Nuclear Intruments and Methods A

Geneva, Switzerland

May 11, 2001

* On leave of absence from INFN, Sezione di Padova, Via Marzolo 8, I-35131, Padova, Italy
† On leave of absence from INFN, Sezione di Milano, Via Celoria 16, I-20133 Milan, Italy

1 Introduction

The CNGS project is to send a beam of neutrinos from CERN to detectors in the Gran Sasso Underground laboratory (LNGS) over a distance of 732 Km. The overall project is described in a Conceptual Technical Design Report [1]. An Addendum to this report gives details of the secondary beam parameters that are used in this study[1] [2].

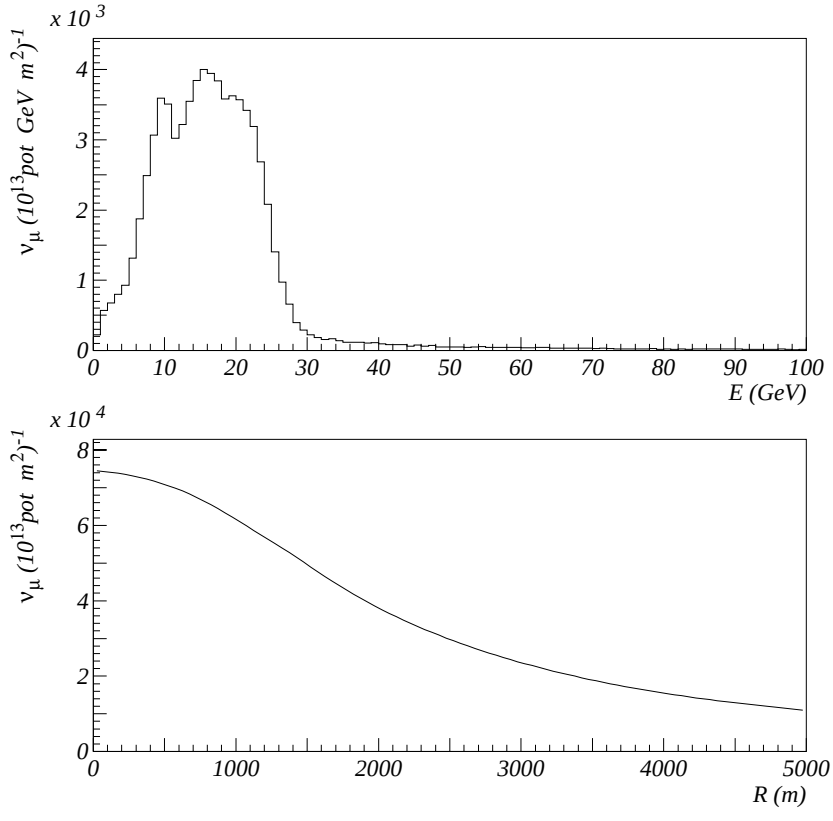

Figure 1: *Energy and radial distributions of the CNGS ν_μ flux at Gran Sasso (732 Km from target) for the fully aligned beam line.*

The expected energy and radial distributions of muon neutrinos at Gran Sasso are shown in Fig. 1. In the forward direction the expected tau neutrino charged current (CC) event rate follows closely the shape of the muon neutrino energy distribution. There is an essentially flat top of some 500 m in radius at LNGS whilst the detector caverns extend over about 100 m in the radial plane: it follows that the neutrino beam direction has to be established with an accuracy better than 0.5 mrad. The geodesic alignment of the beam line is expected to be $\sim$0.05 mrad.

The current beam is optimized for neutrino-tau appearance experiments: the figure of merit in the design is taken to be the expected ν_τ charged CC event rate at Gran Sasso in the 0-100 GeV energy range. Results of simulations for different values of Δm^2 and for $sin^2(2\theta) = 1$ are given in Table 1; the nominal value of 4.5×10^{19} protons on target per year and 100 % detector efficiency have been assumed.

A schematic layout of the beam elements at the CERN site is shown in Fig. 2. The target is a series of cylindrical graphite rods (4 mm diameter) with variable spacing, cooled by helium gas. The

[1] Whilst the CNGS beam has been further improved recently [3], all comparisons are referenced to beam parameters of this Addendum except for the proton beam size and divergence at focal point, which have been set to the more realistic values of $\sigma_{x,y}$ = 0.53 mm and $\sigma_{\theta x,y}$ = 0.053 mrad. The other changes do not affect the conclusions of this note.

Energy range E_{ν_τ} [GeV]	1 - 30	1 - 100
$\Delta m^2 = 1 \times 10^{-3}$ eV^2	2.34	2.48
$\Delta m^2 = 3 \times 10^{-3}$ eV^2	20.7	21.4
$\Delta m^2 = 5 \times 10^{-3}$ eV^2	55.9	57.7
$\Delta m^2 = 1 \times 10^{-2}$ eV^2	195	202

Table 1: *Expected number of ν_τ CC events at Gran Sasso per kiloton per year assuming 4.5×10^{19} protons on target per year and 100 % detector efficiency.*

focusing elements in a wide energy band neutrino beam, the horn and the reflector, are toroidal lenses with a magnetic field between the inner and outer coaxial conductors: the inner conductors are shaped to provide the desired focusing effect (see Appendix B). Collimators between the active elements are filled with helium gas to reduce absorption and scattering of the secondary particles. After the beam cavern, 100 m from the target, there is an evacuated decay tunnel of $\simeq$1000 m length and 2.54 m diameter followed by a graphite and steel shielding (4×4 m^2 in cross-section) that is designed to stop all hadrons. The optical system is cylindrically symmetric about the nominal beam axis.

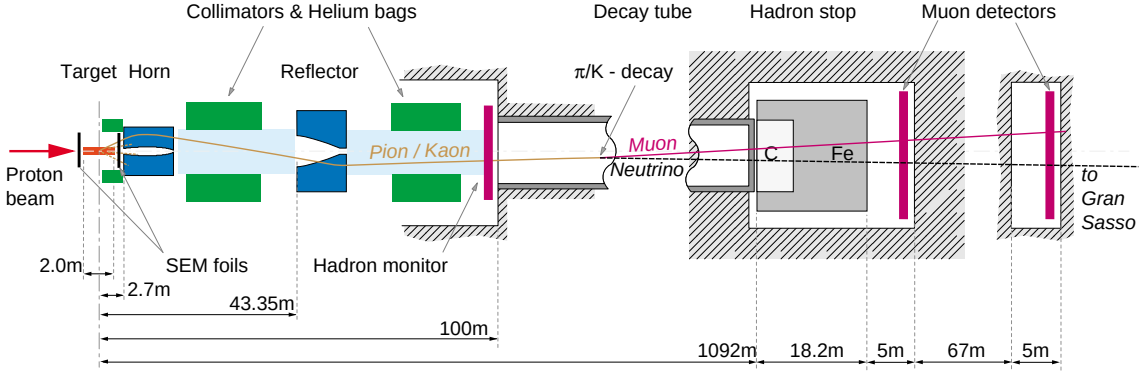

Figure 2: *Schematic layout of the CNGS elements at the CERN site.*

Beam *position monitors* are foreseen throughout the proton beam line and in particular at the upstream and downstream ends of the target enclosure. Two *muon detector chambers* are foreseen: the first chamber is located just after the hadron stop shielding, the second is placed 67 m downstream in the molasse rock. A further *"hadron monitor"* has been considered in front of the decay tube to monitor the secondary charged particles flux. In addition, large area *muon monitoring planes* at Gran Sasso are suggested which would detect muons induced by neutrino interactions in the rock upstream of the experimental caverns.

2 The simulation programs for the CNGS beam-line

In order to compute the neutrino beam spectra at Gran Sasso and the effects of misalignments, three independent Monte Carlo simulations of the CNGS beam-line have been set-up.

Two of them are full simulations both relying on the FLUKA [4, 5] code for the production of secondary particles in the target. The transport of particles through the CNGS layout is performed either by FLUKA or by NEOBEAM [6] which is an application of the GEANT3 package [7].

The third program is a fast simulation stand-alone FORTRAN code, based on a parameterization of the secondary particle production in the target, followed by a biased tracking and decay of secondary mesons [8].

A more detailed description of the simulation codes is presented in Appendix A. Rapid studies of neutrino spectra and alignment effects have been performed with the fast simulation program; the full Monte Carlo codes have been used to improve the confidence level of our conclusions. Their predictions are in very good agreement as shown later in this note.

Beam profiles are recorded at the monitor positions in a plane orthogonal to the beam (z) axis. Mesons and muons are tracked down to a kinetic energy of 10 MeV. The radius of the detector areas are 1.25 m for the "hadron monitor" and 3 m for the two muon chambers. The system is cylindrically symmetric but, by convention, we assume that misalignments occur in the x-axis direction. Beam profiles are shown as projection of the total flux or as particle density (averaged over a width of ± 5 cm) across the x-axis. Only the central region of the profiles is shown, where most of the flux is concentrated (± 0.6 m for the "hadron monitor" and ± 2 m for the two muon chambers).

The contributions of the electrons and photons and their effects at the muon monitors are not taken into account. In Section 4 and 5, their effect on the sensitivity of the "hadron monitor" and of the "Secondary Emission Monitors" is discussed.

3 Effect of alignment errors

The aligned beam profiles at the monitors are shown is Fig. 3. Full and fast symulations give identical results, within statistical errors, in terms of neutrino beams and secondary particle fluxes at the "hadron monitor". Due to the simplified tracking of muons in the shielding, which is used in the fast symulation, the absolute muon rates at the muon chamber locations differ by at most 10 % but the shape remain the same. The level of the agreement remains the same in misaligned profiles comparisons.

The particle intensities are shown in Table 2. Note that at the "hadron monitor" the peak intensity in Table 2 (given with 1 cm^2 resolution) does not coincide with that visible in Fig. 3 because in the latter the uncollided proton peak ($\simeq 6$ % of the primary beam) is smeared by the 5 cm adopted resolution.

monitors	total flux /10^{13}pot	peak flux /cm^2/10^{13}pot
"hadron"	1.3 10^{13}	5.1 10^{10}
first muon chamber	8.1 10^{11}	2.2 10^{7}
second muon chamber	2.5 10^{10}	3.3 10^{5}

Table 2: *CNGS secondary beam fluxes (charged particles) at the different monitors estimated with the full Monte Carlo simulations. Electrons/photons have not been taken into account. Mesons and muons are tracked down to a kinetic energy of 10 MeV.*

Several sources of beam errors have been studied in this note[2]:

- Lateral displacements of beam line elements (proton beam, horn and reflector)
- Angular displacements of the proton beam
- Changes of divergence of the proton beam
- Geodesic misalignment of the whole beam line

In the following subsections, these errors are described in detail.

3.1 Lateral displacement of the proton beam at the target

The position of the proton beam at the target is expected to be accurate to 0.1 mm. We have studied cases where the proton beam is displaced by up to 1.5 mm parallel to the reference axis.

[2] Another study was performed by the ICANOE collaboration mostly aimed at evaluating the systematic errors in the beam contamination [9]. Their results agree with those presented in this note.

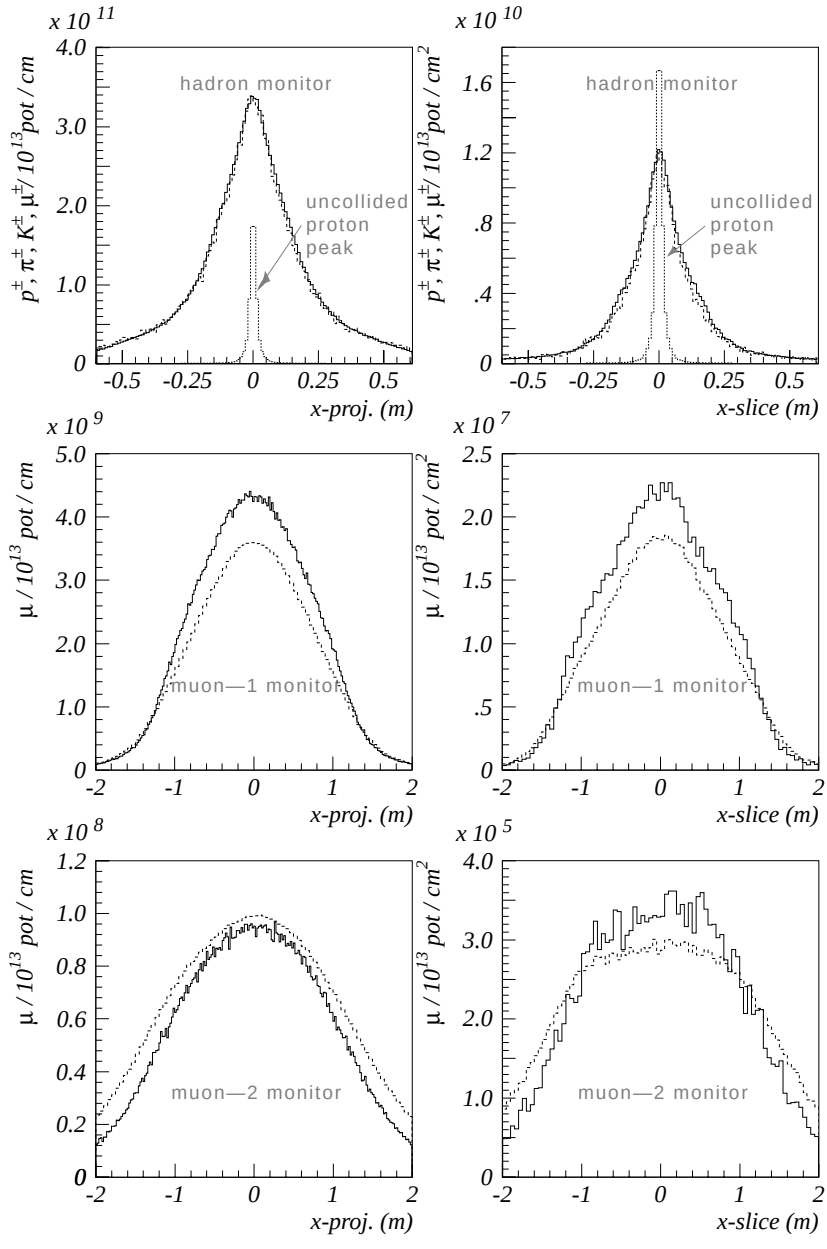

Figure 3: *CNGS secondary beam profiles for the fully aligned case: solid lines are from the full Monte Carlo simulation, dashed lines are from the fast simulation. On the left: projection profiles over the full detector area; on the right: slice profiles (averaged over a width of* ± 5 *cm). At the "hadron monitor" the uncollided proton peak (*$\simeq 6\%$ *of the primary beam) is smeared by the 5 cm resolution (the unsmeared radial distributions are shown in Fig. 6); it is shown separately because its profile depends on the primary beam size and divergence and not on the focusing optics.*

Displacements larger than 1.0 mm are needed to affect the number of ν_τ CC events at Gran Sasso as shown in Table 3 and Fig. 4. This is mainly because a sizable fraction of the proton beam does not intercept the target. There is also a small increase of $\bar{\nu}_\mu$ CC events which does not effect the LNGS detectors performance [10]. No effect is seen at the hadron monitor. The muon monitors are sensitive to these displacements. At the second muon monitor, the maximum displacement and distortion of the profile distribution is detected. This is a combined result of the optics and the energy loss in the molasse rock.

	ν_τ CC events normalized (%)	Hadron monitor X_{slice} (cm)	First muon chamber X_{slice} (cm)	Second muon chamber X_{slice} (cm)
horn lateral displacement				
3 mm	99.0	1.4	10.1	-0.6
6 mm	97.2	2.7	19.1	-3.5
9 mm	93.8	3.8	24.3	-4.6
reflector lateral displacement				
10 mm	99.6	1.0	5.7	-10.7
20 mm	98.4	1.8	14.7	-12.6
30 mm	97.0	2.5	21.5	-18.8
proton beam lateral displacement				
0.5 mm	100.3	-0.1	-0.6	7.3
1.0 mm	97.2	-0.1	-1.2	14.8
1.5 mm*	83.0	0.0	-2.0	19.6
proton beam angular displacement				
0.5 mrad	100.0	1.2	-1.2	3.7
1.0 mrad	98.7	2.4	2.3	10.4
statistical error				
σ_{stat}	0.2	0.1	0.5	1.2

Table 3: *Variations in X_{slice} for various misalignment cases. X_{slice} is the average of the x-slice histograms. The ν_τ CC event rate at Gran Sasso is given normalized to the expectation for the perfectly aligned beam (21.4 events/kt/year for $\Delta m^2 = 3 \times 10^{-3}$ eV^2 and full mixing). *Note that, in the case of 1.5 mm lateral displacement of the proton beam, a sizable fraction does not intercept the target.*

3.2 Angular displacement of the proton beam at the focal point

The proton beam is designed to be focused at 50 cm inside of the target and the beam steering system allows angular displacement of the beam axis around this point. A resolution of 0.1 mrad is expected. We have studied cases where the proton beam has angular displacements up to 1 mrad with respect to the Z-axis. The number of ν_τ CC events at Gran Sasso is found to be not very sensitive to misalignments even in the unrealistic case of 1 mrad. The second muon monitor is always more sensitive than the other two detectors. The displacement of the beam profile distribution is in the opposite direction to the misalignment.

3.3 Change of divergence of the proton beam

At a given momentum (400 GeV/c) the emittance of the proton beam at the target is fixed. However, the size and divergence can be altered by changing the focusing parameters. We have studied the case where the divergence is doubled and the spot size is halved[3]. The number of ν_τ CC events and the beam profiles are insensitive to this change. At the "hadron monitor" the uncollided proton peak is considerably reduced (by nearly 50 %).

3.4 Lateral displacements of the magnetic lenses

The co-axial lenses used to focus the secondary particles, horn and reflector, could be misaligned. The expected position resolution is 0.1 mm. We have studied cases where a displacement of the horn by Δx up to 9 mm parallel to the beam (Z) axis occurs. Displacements of the reflector up to 3 cm have also been considered.

[3]Note that the references values are $\sigma_{\theta x,y} = 0.053$ mrad and $\sigma_{x,y} = 0.53$ mm.

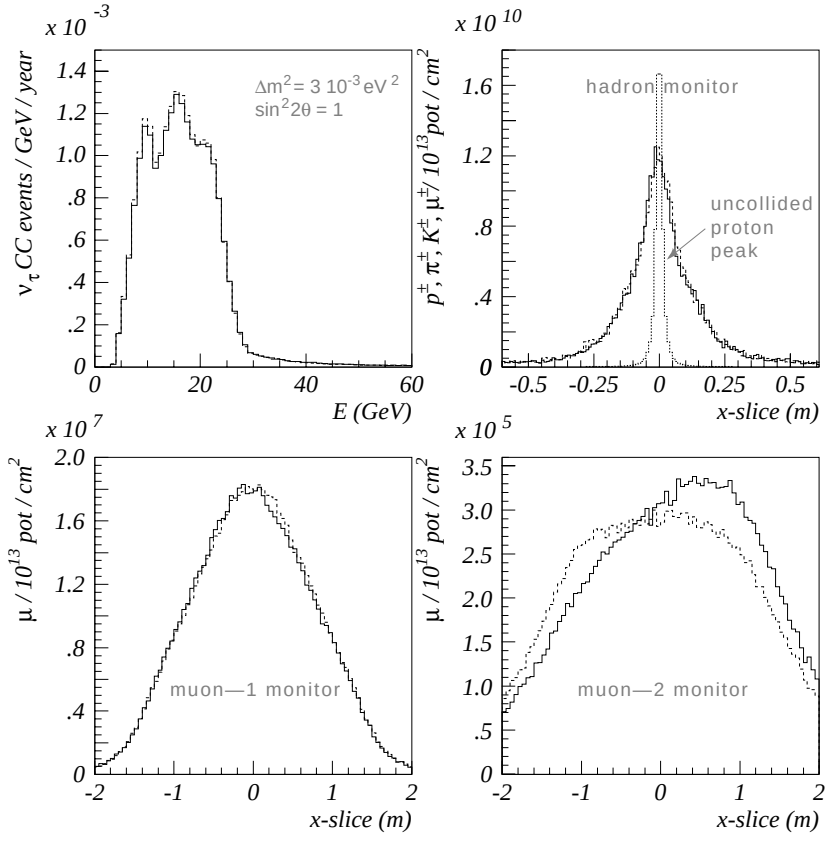

Figure 4: *Proton beam lateral displacements of Δx = 1 mm: ν_τ CC events and profile distributions. For comparison the fully aligned case is also shown (dashed lines). Profiles are from the fast simulation.*

In the case of horn displacements, the number of ν_τ CC events is sensitive to misalignments only above $\Delta x = 6$ mm where the reduction is about 3 %. At the monitors, there is a dramatic distortion in the shape of the beam profiles with a consequent shift in the mean value. This is shown in Table 3 and Fig. 5. Equivalently displacements of the reflector larger than 2 cm are needed to significantly reduce the ν_τ CC events rate at Gran Sasso.

Similar results are found in case of angular misalignments leading to displacements of the horn and/or reflector "necks" only [10].

3.5 Geodesic misalignment of the whole beam system

The geodesic alignment of the whole beam-line (proton beam-target-lenses-decay tunnel-muon chambers) is expected to have an accuracy of 0.05 mrad. We have studied the case where a huge misalignment of 0.5 mrad with respect to the reference Gran Sasso direction occurs. This corresponds to 360 m off-axis at LNGS. The number of ν_τ CC events is reduced only by 2.5 %. Clearly, no effect is expected at the monitors at CERN. Monitors at LNGS are best suited to detect such a misalignment (see Section 6).

4 Sensitivity of the "hadron monitor"

A prototype "hadron monitor", consisting of an array of simple ionization chambers, had been installed just upstream of the decay tunnel during the later running the WANF [11] beam at CERN. We have investigated the use of such a monitor in the CNGS beam line. Results presented in Section 3 show that

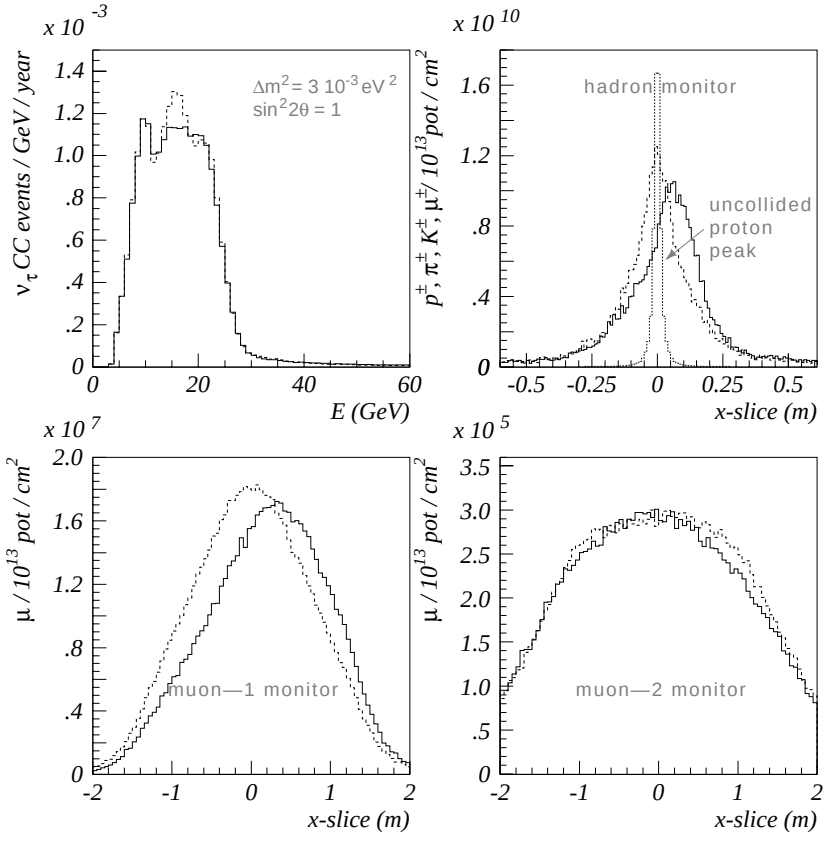

Figure 5: *Horn lateral displacements of $\Delta x = 6$ mm: ν_τ CC events and profile distributions. For comparison the fully aligned case is also shown (dashed lines). Profiles are from the fast simulation. Note that at the "hadron monitor" the uncollided proton peak is not affected by the horn displacement.*

it would be particularly sensitive to displacements of the horn and reflector. In addition, the integrated ionization signal intensity could give a first estimation of the total meson flux entering the decay tunnel which is linked to the neutrino flux intensity. However, such an unshielded monitor will detect ionization induced by all charged particles down to very low energies.

A Monte Carlo simulation of the neutrino beam line was carried out, based on the FLUKA stand-alone code [4]. Charged and neutral particles produced with kinetic energy higher than 30 MeV in any material along the beam line were tracked down to very low energy, 1 MeV for electrons/photons and 10 MeV for all other particles.

The results are quite discouraging. They show that the sensitivity is strongly limited by the large electron/positron flux from electro-magnetic showers. The radial distribution of charged particles is dominated by electro-magnetic components and is relatively flat within the nominal acceptance of the focusing optics (up to a radius of 60 cm) as shown in Fig. 6. These particles are mostly of very low energy and are produced in interactions all along the beam line, hence the directionality of the primary beam is obscured. Only the narrow uncollided proton peak hardly emerges from the electron/photon background and this is unaffected by displacements of the horn or reflector. In addition the radial size and amplitude of the proton peak are strongly dependant on the divergence of the primary beam which might ultimately be chosen for beam operations.

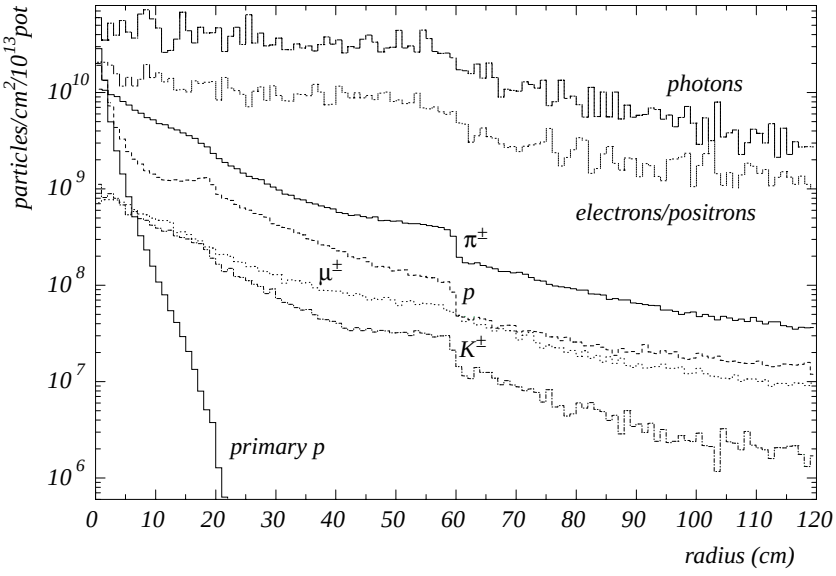

Figure 6: *Radial distribution of secondary particles at the "hadron monitor" location. Electro-magnetic components, shown separately, are clearly the dominant signals.*

5 Secondary emission monitors at the target

An accurate alignment of the primary proton beam with the CNGS long, thin target[4] is important to ensure the maximum number of interactions within the target and is a precondition of alignments in the secondary hadron beam.

A standard method to check the alignment is to use segmented secondary emission (SEM) foils before and after the target. The ratio of the "sum" signals (downstream/upstream) gives the secondary particle multiplicity which is a measure of the interaction rate. The upstream SEM is used to measure the proton beam intensity before the target. The left–right and up–down signals indicate the direction and magnitude of mis-steering of the proton beam.

A FLUKA stand-alone [4] simulation has been set-up to estimate the sensitivity of this method to parallel displacements and angular rotations of the primary proton beam. Mesons have been generated assuming the spatial and angular distribution of protons at the focal point (see Section 3.3). Secondary pions, kaons, muons and protons with momentum p $\geq$ 10 MeV/c are recorded 15 cm downstream of the target within a circular area of 1 to 3 cm diameter subdivided into four sectors (up, down, left and right).

The material structure of the target box and supports used in the WANF (see Appendix C) has been also included in the simulation in order to get an estimation of the effects of the electron/photon background on the sensitivity of the measurement. For this purpose electrons and gammas with momentum down to 1 MeV and 2 MeV respectively are also recorded even if they are not expected to worsen significantly the sensitivity because they are produced with similar kinematics.

In Table 4 the total number of hadrons, electrons and gammas normalized to one proton on target is shown for various diameters of the SEM foils in the case of fully aligned beam. Despite the high rate, the gamma halo is expected to give a negligible counting rate in a SEM detector because the SEM foils are extremely thin (a fraction of a millimeter).

Asymmetries in the space distribution of the charged particles are detected combining left–right and up–down sectors. A parallel displacement Δx of the primary proton direction with respect to the

[4]The CNGS target is about 2 m long and is made of 8 graphite rods (10 cm length, 4 mm diameter) spaced by 9 cm plus an additional rod at the end of 50 cm length.

	P-threshold (MeV/c)	particles/pot		
		$\phi = 1$ cm	$\phi = 2$ cm	$\phi = 3$ cm
$h^{\pm}$	10.	0.6	1.5	2.2
n	10.	0.1	0.2	0.3
$e^{\pm}$	1.	1.3	2.7	3.9
γ	2.	4.7	8.0	9.8

Table 4: *Rate of charged hadrons ($h^{\pm}$), neutrons (n), electrons ($e^{\pm}$) and gammas (γ) with momentum above the threshold defined in the first column, crossing SEM's with different diameters, ϕ, in the case of fully aligned beam.*

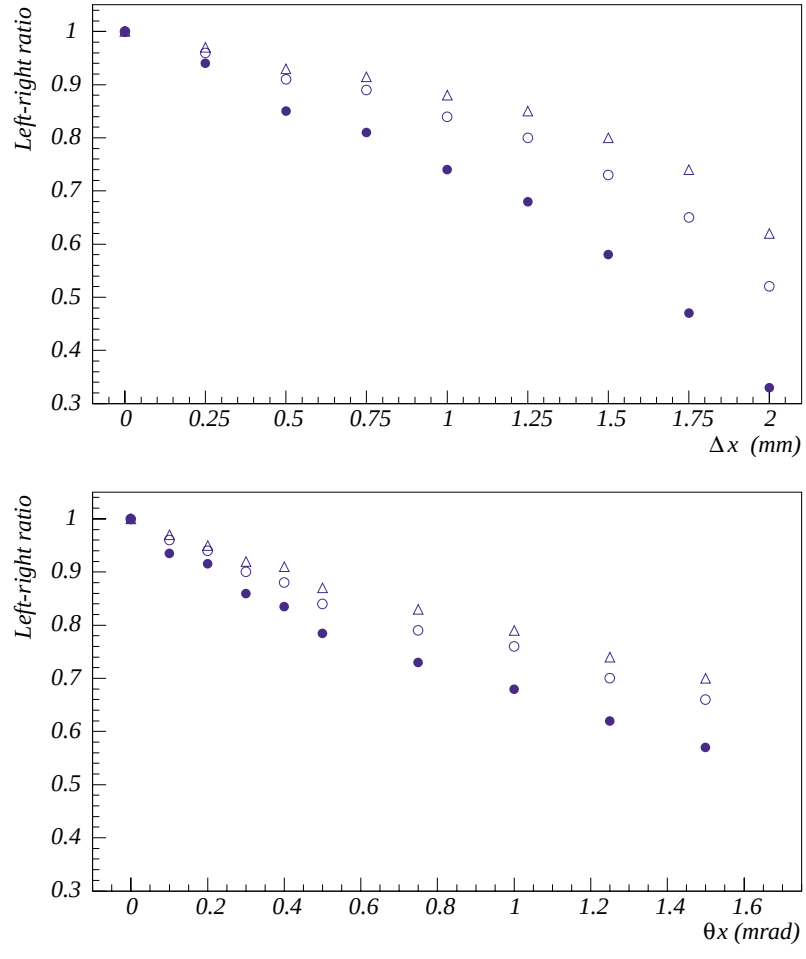

Figure 7: *Left–right counting rate ratio in the downstream SEM foils as a function of the beam parallel displacement Δx (top) and of the steering angle θx (bottom) for foils of different diameter: 1 cm (•), 2 cm (○) and 3 cm (△).*

target axis produces a large asymmetry in the particle flux. An effect of 6% is detected in the left–right counting rate ratio for $\Delta x = 0.25$ mm (Fig. 7) if a recording diameter of 1 cm is used. Differences larger than 20% are observed for displacement of the primary protons beam exceeding 1 mm.

Similarly, a 8% difference in the left–right counting ratio is measured when the proton beam is mis-steered in the x-z plane, centered at the target focal point, by an angle $\theta_X = 0.2$ mrad. In addition no major change in the total particle multiplicity is observed.

Larger diameters of the recording SEM provide less sensitive measurements, although statistically significant, of the asymmetries due to a larger contribution of the very low energy electron/photon background.

This study shows that a segmented Secondary Emission Monitor, placed 15 cm downstream of the target, would be sensitive to small misalignments of the primary proton beam and complements the information obtained at the muon monitors. Small diameter detectors ($\simeq 1$ cm) are preferable to minimize the contribution of the diffused electron/photon background.

6 Beam monitoring at Gran Sasso

The implementation of a beam monitoring device at the Gran Sasso Laboratory, able to provide information about the neutrino flux in "real-time", would be a useful feedback not only during the setting up phase but also during normal operation to check to long term beam stability.

In principle the experiments at LNGS could provide such information by counting the number of ν_μ charged current (CC) interactions. Unfortunately, this could take months to accumulate due to their limited mass and their complexity.

On the other hand, large area muon detectors could be easily realized by means of RPC planes or streamer tubes placed perpendicularly to the beam direction and close to the up-stream wall of the three experimental halls of LNGS. These detectors could be as large as $13 \times 13\,\mathrm{m}^2$ and would count crossing muons induced by ν_μ CC interactions in the rock up-stream of the laboratory. In time coincidence with the CNGS beam spill, the measurement could be practically background free. Given that the muons are highly penetrating particles, this counting technique takes advantage of a very large rock depth in front of the experimental halls at LNGS.

In the case of CNGS, with neutrino energies in the 10-30 GeV range, the useful depth is several tens of meters equivalent to a mass larger than 10 kt. About 0.86 muons/m^2/day are expected to emerge from the rock up-stream of the LNGS experimental halls, their energy spectrum is shown in Fig. 8. This muon counting technique can provide the beam intensity with statistical error of few percent within less than a week: 29000 events per year (145 events per day) are expected over a $13 \times 13\,\mathrm{m}^2$ detector. Note that the spectrum presented in Fig. 8 differs from that of Reference [3] because here the energy loss of the muons in the rocks has been included; in addition the spectrum in [3] is due to the updated neutrino spectrum which is slightly more energetic than that used in this paper.

To first approximation, the muon counting rate is insensitive to variations in the rock density: a decrease in density gives less interactions but this is compensated by an equivalent increase in the muon range and hence reduced filtering. The estimated sensitivity of this measurement to extreme alignment errors in the CNGS beam line is shown in Table 5.

	ν_μ CC int. (%)	ν_τ CC int. (%)	μ_{rock} (%)
Standard CNGS beam	100.0	100.0	100.0
Proton lateral displ. (1 mm)	98.3	97.2	99.5
Proton angular displ. (1 mrad)	98.2	98.7	97.6
Horn displacement (6 mm)	98.4	97.2	99.9
Geodesic misalignment (360 m)	97.0	97.5	97.8

Table 5: *Variations in the number of crossing muons from ν_μ interactions in the rock observable in a large area detector at Gran Sasso, for some extreme cases of alignment errors. In case of perfectly aligned beam the expected absolute rates are: 2.45 10^3 ν_μ CC events/kt/year, 21.4 ν_τ CC events/kt/year (for $\Delta m^2 = 3 \times 10^{-3}$ eV^2 and full mixing) and 171 μ_{rock}/m^2/year.*

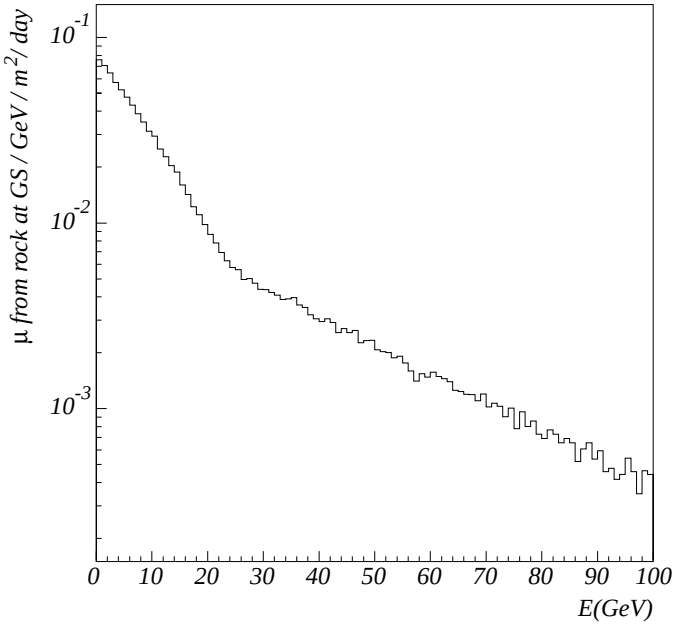

Figure 8: *Energy spectrum of muons from ν_μ interactions emerging from the rock upstream of the Gran Sasso halls observed in a large area detector (muon energy loss in the rock has been included).*

7 Conclusion

The results of this study show that, except for extreme misalignments of beam elements or mis-steering of the beam, no significant changes in the ν_τ event rate are seen at Gran Sasso. Given the alignment accuracy which is expected to be achieved, no effect will be observable both at the monitors at CERN and at Gran Sasso. This somewhat unexpected conclusion is explained mostly by the large diameter of the decay tunnel which represents the main aperture stop in the optical system. It follows that remote position adjustments of the horn and reflector during run-time appear to be unnecessary: manual adjustments for the initial geodesic alignment of these elements are adequate.

Concerning the proton beam, a word of caution is mandatory: while the accuracy requested in terms of CNGS performance for steering the proton beam is very modest, aspects of radio-protection and, more generally, protection of material in the target chamber, require that the proton beam position and angle at the target be very well controlled. The upstream and downstream SEM monitors at the target are essential for the beam adjustment and must have good sensitivity. Remote adjustments of the target in position and angle are foreseen.

The use of the so called "hadron monitor" in front of the decay tunnel could have provided useful information but any signal would be swamped by the low energy electron/photon background except for a narrow peak due to the uncollided primary protons. At present, no technical solution is envisaged.

The monitors in the muon chambers are sensitive to mis-alignments in the proton beam and focusing system. The profiles obtained will determine the "granularity" needed in the muon monitors. The monitor planes should be installed at the downstream side of the chambers in order to avoid that electrons, coming from muon bremsstrahlung interactions in the upstream shielding material, are added to the muon signal.

Muon monitor planes in the caverns at Gran Sasso will give a good indication of the overall system alignment and neutrino beam intensity. Information from these monitors will be available on a much faster time-scale than that obtained from the neutrino detectors.

Finally, the most critical requirement is that the geodesic alignment of the beam system and decay tunnel at CERN towards the Gran Sasso is correctly established. An alignment precision of about 0.1 mrad is desirable: a significant, but not dramatic effect is seen with a misalignment of 0.5 mrad. The geodesic services expect to obtain a precision of 0.05 mrad using well known reference points in the SPS and LEP/LHC tunnels and at Gran Sasso.

8 Acknowledgements

We would like to thank the other members of the CNGS Secondary Beam Working Group [12] for their valued comments.

References

[1] G. Acquistapace et al., *NGS Conceptual Technical Design*, CERN 98-02; INFN/AE-98/05, 1998

[2] R. Bailey et al., *Addendum: The CERN Neutrino Beam to Gran Sasso*, CERN-SL/99-034(DI); INFN/AE-99/05, 1999

[3] A.E. Ball et al., *CNGS: Update on secondary beam layout*, CERN SL-Note-2000-063 DI; 2000

[4] G. Collazuol et al., *Hadronic models and experimental data for the neutrino beam production*, Nucl. Instr. Meth. A449 (2000) 609

[5] A. Fassò, A. Ferrari, J. Ranft, P.R. Sala, *Electron-photon transport in FLUKA: status* and *FLUKA: Status and Perspectives for Hadronic Applications*, invited talks at the "Monte Carlo 2000" conference, Lisbon, Oct. 2000, proceedings in Press, see also http://www.cern.ch/fluka

[6] A.E. Ball, S. Katsanevas, N. Vassilopoulos, *Design Studies for a Long Base-Line Neutrino Beam*, Nucl. Inst. Meth. A383 (1996) 277-290 and N. Vassilopoulos, private communication

[7] GEANT3.21, The CERN program library

[8] M. Bonesini, A. Marchionni, F. Pietropaolo, T. Tabarelli de Fatis, *On particle production for high energy neutrino beams*, in Press on Eur. Phys. J. C, CERN-SL-2001-005 and hep-ph/0101163

[9] F. Cavanna et al. (the ICANOE collaboration), *ICANOE: Answers to Questions and Remarks Concerning the ICANOE Project*, LNGS-P21/99-ADD2, CERN/SPSC 99-40, SPSC/P314 Add. 2 (1999).

[10] CNGS Secondary Beam Working Group Minutes, F. Pietropaolo and N. Vassilopoulos, private communication

[11] G. Acquistapace et al., CERN-ECP/95-14, 1995

[12] http://proj-cngs.web.cern.ch/proj-cngs/ProjectOrganization/CNGSSBWG.htm

[13] A.E. Ball et al., *Update Results of the Horn Study for the Neutrino Factory*, Proceedings of the DOE/ECFA/ICFA/NSF Workshop "Muon Storage Ring for a Neutrino Factory" (vfact'00), Monterey, CA, USA, to be published in Nucl. Inst. Meth A

[14] G. Ambrosini et al., *Measurement of charged particle production from 450 GeV/c protons on beryllium*, Eur. Phys. J. C10 (1999) 4, 605

A Simulation Programs

A.1 The full simulations of neutrino beams

The standalone FLUKA code is capable of handling transport and interactions of hadronic and electromagnetic particles in any material over a wide energy range, from thermal neutrons to cosmic rays. It is intrinsecally an analogue code, but can be run in biased mode for a variety of deep penetration applications. Biasing of penetration and decay has been used in the simulations presented here to enhance the statistics at Gran Sasso and in the muon detectors.

Details of the code and comparisons with experimental data can be found in the literature. In particular, the very nice agreement with particle production data at the energy of interest for CNGS [4] ensure the reliability of the CNGS simulations.

The NEOBEAM (NEutrino Oscillation BEAM) simulation code is an application of the GEANT 3 package and is made to design and study neutrino beams. It has been used to optimize the layout of neutrino beam elements such as targets and focusing devices, to study the distributions of secondary particles at different locations throughout the beam layout and finally to calculate the expected neutrino spectra at any distance from the source. In the case of CNGS beam line, the FLUKA code is used to generate secondary particles in proton-target hadronic interactions. The beam geometry and the tracking is done in the framework of GEANT package.

The program has been used not only in the design studies of CNGS but also for a number of other issues. Among them, several neutrino beams to Gran Sasso and NESTOR laboratories as described in ref. [6], some WANF simulations and a pion collection system for the proposed the CERN neutrino factory [13].

A.2 The fast simulation of neutrino beams

The fast stand-alone code was developed as a tool that allows varying and optimizing all elements and the geometry (in 3-D) of neutrino beam lines. It provides results in terms of neutrino spectra and distributions at any distance with high statistics and in short time. The program also provides spectra and distributions of secondary hadrons and muons at monitor locations.

It is based on the parameterization of the secondary meson production from protons onto a thin target as proposed in ref. [8] and referred to as "BMPT parameterization". It extends its prediction over a wide range of momenta and of secondary particles. The sizable fraction of tertiary production from re-interactions in the target and downstream material is also evaluated from experimental data [14].

In order to speed up the calculations of neutrino spectra at large distances over a small solid angle ($\Omega \simeq 10^{-10}$ rad for the future LBL beams at CERN and FNAL) all mesons are forced to decay along the beam line emitting a neutrino that in turn is forced to cross the detector. A weight is then assigned to each neutrino, proportional to the probability that this process actually happens. This method is implemented by subdividing the simulation into subsequent steps. The weight assigned to each neutrino is the product of the probability originated in each step multiplied by the solid angle subtended by the detector:

$$W_{tot} = \Pi(W_i)\Omega_{det}. \tag{1}$$

In the following we briefly review and explain the various factors in the above formula.

– *Meson production along target.* – Secondary mesons are generated along the target according to the distribution of the proton interaction points. The latter depends on the proton beam size and divergence, on the target thickness, T_{targ}, and on the proton interaction length, λ_p, of the target material. Protons are forced to interact in the target. Yield, momentum and angular distributions of the mesons are given by the BMPT parameterization. These numbers depend on target material, density and length and on the number of protons on target.

Meson trajectories, $z'(z,\theta)$, in the target are calculated and used to estimate the probability that the mesons, with interaction length λ_s exit the target without re-interacting. The associated weight is:

$$W_1 = (1 - e^{-T_{targ}/\lambda_p})e^{-z'/\lambda_s} \quad (2)$$

Tertiary production due to re-interactions of secondaries in the target is added following the rules proposed in the BMPT parameterization; as an example, in the case of continous target we have:

$$W_2 = 1 + A_{ter}(1 - p/p_{max})^{b_{ter}}(1 - e^{-\lambda_{ter}/z})z/\lambda_p \quad (3)$$

where A_{ter}, b_{ter} and λ_{ter} are phenomenological parameters defined in ref. [8].

– *Meson tracking in the neutrino beam-line*. – The trajectory of each meson in the beam-line is calculated, taking into account the tracking in the magnetic field of horn and reflector, until it hits the walls of the decay tunnel or the collimators. The amount of material crossed by the particle is also recorded. Each meson is forced to decay along its trajectory, $traj$, accordingly to its decay length, λ_{dec}. The weight associated to this process is:

$$W_3 = (1 - e^{-traj/\lambda_{dec}})e^{-Z_{int}/\lambda_s} \quad (4)$$

where Z_{int} is the material length crossed up to the decay point and λ_s is the interaction length in that material. Meson production from re-interactions in the material along the beam line is taken into account with a weight similar to W_2 in the approximation of short target; namely:

$$W_4 = 1 + A_{ter}(1 - p/p_{max})^{b_{ter}} Z_{int}/\lambda_p \quad (5)$$

– *Neutrino production from mesons*. – For each meson a neutrino is produced; its flavor and its momentum distribution in the parent meson rest frame depend on the decay mode and branching ratio, $B.R.$. The neutrino direction in the laboratory frame is determined requiring that it crosses the detector volume. The angle, $\theta_{s\nu}$, between parent meson and neutrino directions allows calculating the Lorentz boost of the neutrino from the meson rest frame to the laboratory frame. This in turns allows obtaining the neutrino momentum in the laboratory frame. The weight associated to this process is proportional to the probability that the neutrino is emitted in the detector direction. This is obtained by simply boosting back the solid angle subtended by the detector in the meson rest frame, where the neutrino is emitted isotropically:

$$W_5 = B.R. \times (m_s/(E_s - P_s cos\theta_{s\nu}))^2 \quad (6)$$

where m_s, E_s and P_s are the mass, energy and momentum of the secondary meson.

– *Neutrino production from muon decays*. – Muons are produced in the decay of secondary mesons with the appropriate kinematics (branching ratio and polarization). Muons are also tracked through the neutrino beam line and forced to decay to produce neutrinos in the detector direction. Additional weights, $W_{3\mu}$ and $W_5\mu$ (equivalent to W_3 and W_5 for meson decays), are introduced for the neutrinos from muon decay.

Unlike classical unweighted calculations, the statistical accuracy of this method of simulating neutrino beams does not depend strongly on the distance between the detector position and the neutrino source. In the unweighted case, only a fraction of mesons ($\simeq$ 5–10 %) decay before interacting (either in the beam-line material or in the decay tunnel walls); in addition neutrinos are spread over a wide solid angle ($\simeq$ 1 mrad for CNGS) because of the decay kinematics. Hence at large distance the neutrino spectra have to be computed on a surface much wider than the actual detector area, relying on the fact that the spectra shapes vary slowly with the radius. In the CNGS beam, an accuracy better than 1 % can be achieved by tracking the products of several million protons on target and using a detector area of $\sim 10^4$ m^2.

In the parameterization case, since all mesons – within the focusing optics acceptance – are exploited to produce neutrinos in the detector, the statistical accuracy is independent of the detector distance and inversely proportional to the square root of the number of generated positive pions (for ν_μ beams), roughly equivalent to the number of generated proton interactions on target. A statistical accuracy of better than a percent is thus obtained with less than 10^5 p.o.t., for any size of detector surface and any detector distance.

B Ray-tracing graphics for the CNGS wide band neutrino beam

Combined effects of toroidal magnet lenses to produce focusing over a large momentum range:

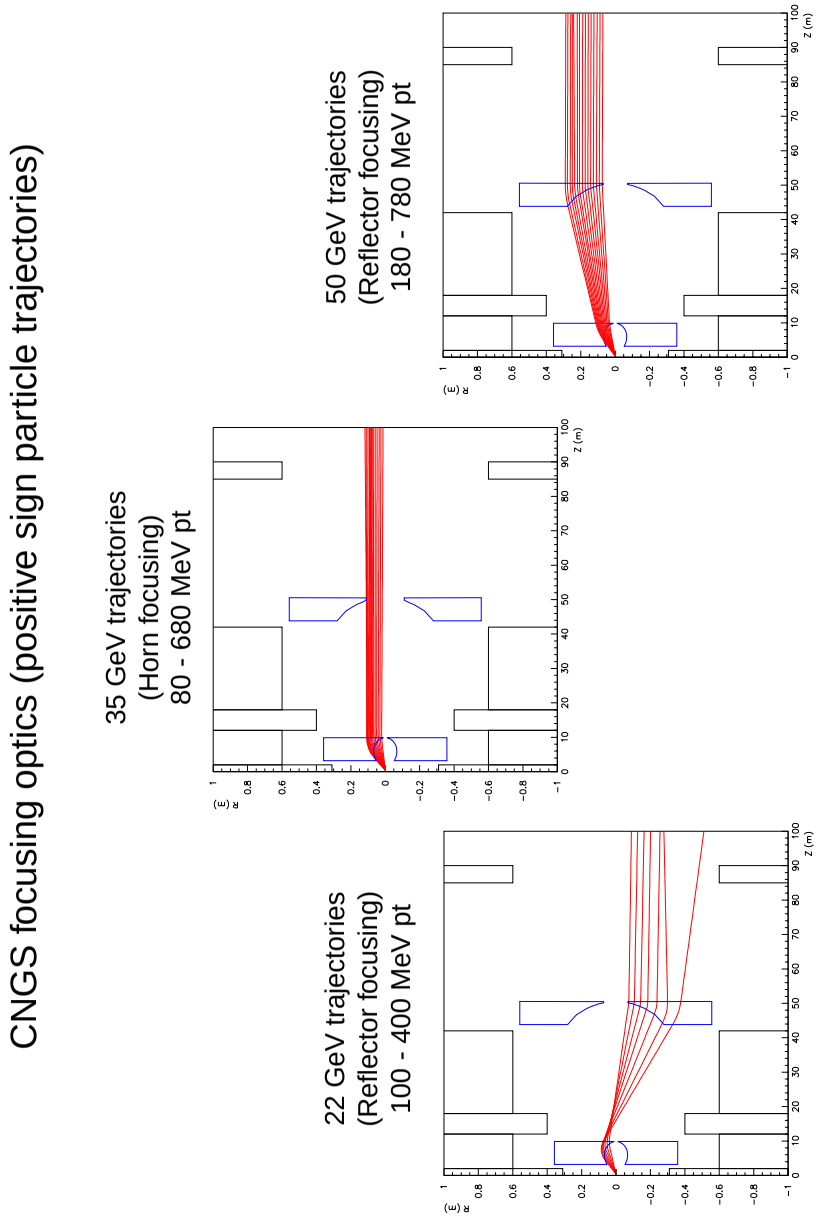

C Support structure in the WANF target box

Schematic drawing of the target rod holders in the WANF target box as included in the full Monte Carlo simulation described in Section 5. The target rods are 10 cm long. The spacing between rods is 9 cm. The supporting carbon plates have a thickness of 2 mm.